Experimental Studies of the Interaction Between a Parallel Shear Flow and a Directionally-Solidifying Front

Meng Zhang
Tony Maxworthy
Department of Aerospace Engineering
University of Southern California
Los Angeles, CA 90089
Email: mengzhan@spock.usc.edu, maxworth@mizar.usc.edu

NASA Grant #: NAG3-1619

Introduction

It has long been recognized that flow in the melt can have a profound influence on the dynamics of a solidifying interface and hence the quality of the solid material[1]. In particular, flow affects the heat and mass transfer, and causes spatial and temporal variations in the flow and melt composition. This results in a crystal with nonuniform physical properties. Flow can be generated by buoyancy, expansion or contraction upon phase change, and thermo-soluto capillary effects. In general, these flows can not be avoided and can have an adverse effect on the stability of the crystal structures. This motivates crystal growth experiments in a microgravity environment, where buoyancy-driven convection is significantly suppressed. However, transient accelerations (g-jitter) caused by the acceleration of the spacecraft can affect the melt, while convection generated from the effects other than buoyancy remain important.

Rather than bemoan the presence of convection as a source of interfacial instability, Hurle in the 1960s suggested that flow in the melt, either forced or natural convection, might be used to stabilize the interface. Delves[2] considered the imposition of both a parabolic velocity profile and a Blasius boundary layer flow over the interface. He concluded that fast stirring could stabilize the interface to perturbations whose wave vector is in the direction of the fluid velocity. Forth and Wheeler[3,4] considered the effect of the asymptotic suction boundary layer profile. They showed that the effect of the shear flow was to generate travelling waves parallel to the flow with a speed proportional to the Reynolds number. There have been few quantitative, experimental works reporting on the coupling effect of fluid flow and morphological instabilities. Huang[5] studied plane Couette flow over cells and dendrites. It was found that this flow could greatly enhance the planar stability and even induce the cell-planar transition. A rotating impeller was buried inside the sample cell, driven by an outside rotating magnet, in order to generate the flow. However, it appears that this was not a well-controlled flow and may also have been unsteady.

Experimental Method

Numerous experiments have been done by other researchers to conduct morphological studies with transparent organic compound growing in a Hele-Shaw cell. The Hele-Shaw cell was used to provide a 2D solidification chamber which made in-situ observations and measurements possible. Furthermore, buoyancy-driven convection is greatly suppressed in a horizontal Hele-Shaw cell so that a microgravity environment can be simulated.

In the present experimental study, we want to study how a forced parallel shear flow in a Hele-Shaw cell interacts with the directionally solidifying crystal interface. The Hele-Shaw cell (figure 1) consists of two parallel quartz glass plates separated by a thin gap (500 μm). Each plate is ground to less than 1/4 wavelength per inch optical flatness. The bottom plate is covered with an aluminium reflective coating, which serves as a front-surface mirror. The top plate has two groups of holes through which liquid alloy can be added or removed. A parallel shear flow is formed by adding liquid into the cell through the holes on one side and removing it through the holes on the other side. The direction of the flow can be reversed by interchanging the inlet and outlet holes. The temperature distribution inside the cell is detected by an embedded Iron-Constantan thermocouple with an accuracy of 0.1°C. The thermocouple is placed next to the incoming flow.

The configuration diagram of the experimental setup is shown in figure 2. It is based on a horizontal Bridgeman furnace. Temperatures of the heater/cooler pair are controlled separately by two water circulators which have temperature stability of up to 0.01°C. A linear temperature profile is set up in the conduction stage. The Hele-Shaw cell, sitting on top of the conduction stage, is driven by a closed-loop micro-actuator to travel back and forth in the direction with the largest temperature gradient. A LEITZ interference microscope is used to observe the microstructure of the S/L interface and to measure the solute concentration field. A flow control system is used to regulate the strength and direction of the flow. This flow system is sealed in a polycarbon box and is maintained at a temperature above the melting point. All the aforementioned parts except the microscope are mounted on a pair of 3D micro-translation stages so that any part of the specimen can be focused.

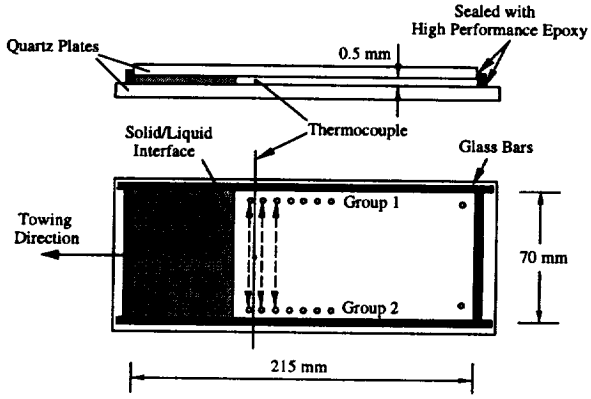

Figure 1 Hele-Shaw cell

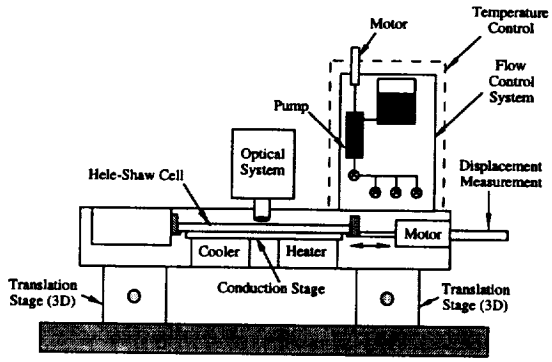

Figure 2 Diagram of the experimental setup

The transparent organic alloy SCN-1.0 Wt% acetone was used as the specimen material because: 1) it has been commonly used in past directional solidification experiment, and 2) its thermophysical properties have been well measured. A set of no-flow experiment were conducted first, during which the Hele-Shaw cell was pulled toward the cold side at some constant speeds (ranged from 3 μm/s to 10 μm/s). The interface evolution and the temperature variation served as a standard for the experiments with flow to compare with. In the second set of experiments, all the experimental condition are the same except the parallel shear flow was started when the planar interface just became unstable (called early applied flow in what follows). Since different pulling speeds will result in different time to instability and different growth rates, the flow was turned on at different times in each experiment. However, the initial cell amplitudes were < 10 μm for all the experiments with early-applied flow. In the third set of experiments, the cellular interface was developed when flow was started (called late applied flow in what follows). The flow temperature was adjusted so that no heat source or sink effect was brought in by the flow. The experiment process was observed in-situ under the interference microscope.

Results and Discussion

Figure 3.a shows the interface morphology changes in a no-flow experiment. The frame code, representing a framing rate of 1/30 second, was started when the Hele-Shaw cell began to move. Since the morphological number M (~130) is much higher than the critical value M_c (1.07) in this case, the S/L interface changed from a planar to a cellular to a dendritic structure. During the entire process, most cells grew in the normal direction to the initial planar interface. For the experiment with early-applied flow shown at figure 3.b, small perturbation existed when the flow was imposed at frame 14865. The flow direction is from top to bottom and flow speed is 15 times higher than the Hele-Shaw cell towing speed. After the flow was imposed, the existing perturbation continued to grow for a short period of time (frame 16068) and then decayed. Eventually the interface returned to a planar state. For the experiment with late-applied flow shown at figure 3.c, the cellular interface was developed when the flow was started at frame 16230. The flow has the same direction and the same strength as the previous one. Unlike the decay observed in figure 3.b, cellular structures started tilting toward the upstream direction. Later secondary dendrites appeared on the downstream side of the leading crystals while the trailing crystals were suppressed. Similar results were obtained when the experiment were repeated at various towing speeds and reversed flow direction.

To further study the parallel shear flow effect quantitatively, the amplitude and the wavelength of the cellular interface were measured at different times during growth for each experimental run. For the experiment with early-applied flow, the planar interface became unstable around a time of 465 second (figure 4.a), after this the perturbation amplitude (A) increased with time (t). Shortly after the flow was imposed at 498 second, the amplitude dropped to zero. The amplitude was 3.8 μm when the flow was turned on. The effect of flow on wavelength (λ) is not as prominent as the effect on amplitude. Figure 4.b shows that the wavelength is nearly invariant before and after the flow. For the case of late-flow experiment as shown in figure 3.c, it is difficult to quantify the

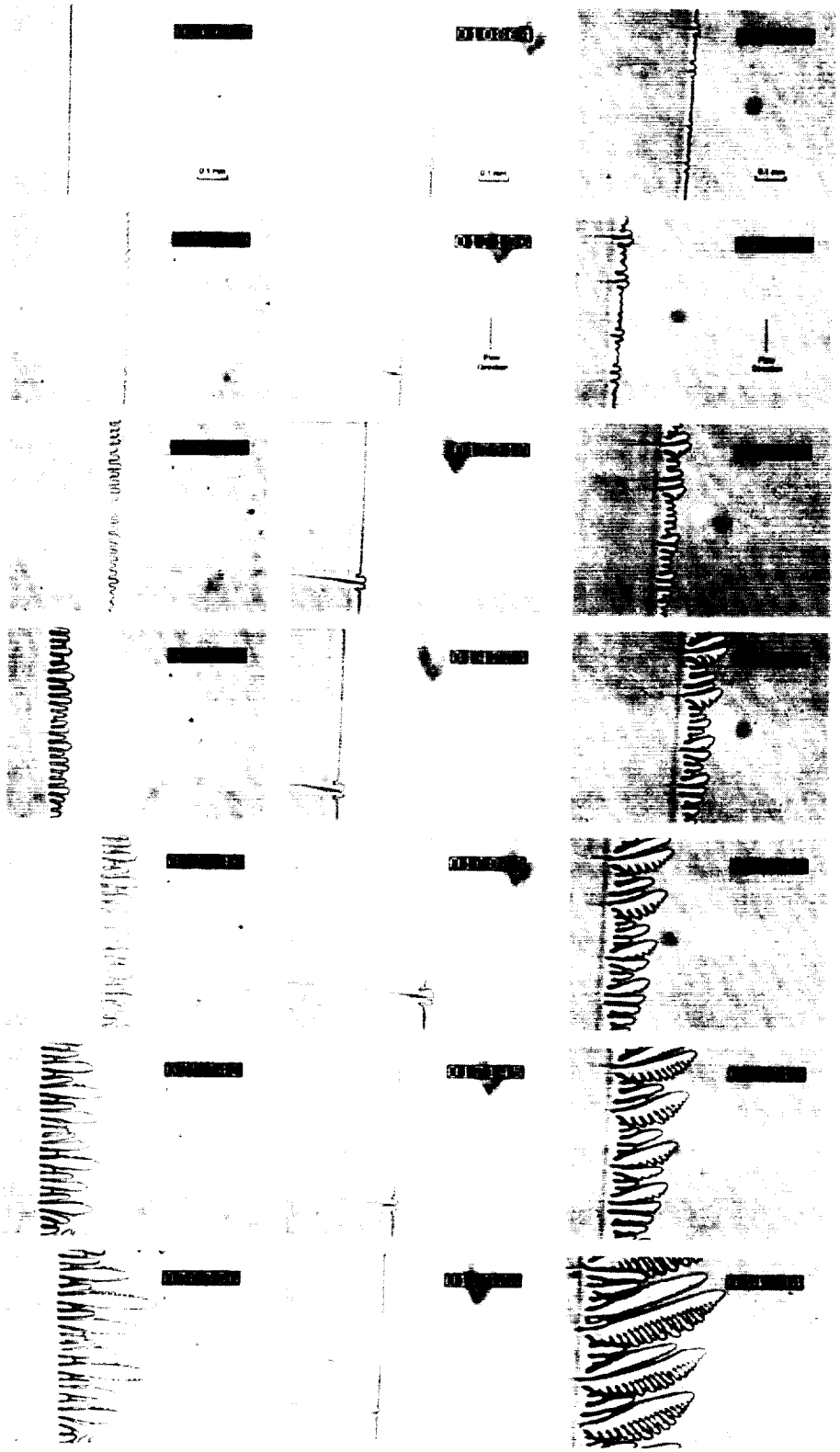

Figure 3 Effect of parallel shear flow on directional solidification interface
a. no flow; b. with early-applied flow; c. with late-applied flow
(towing speed = 4.5 μm/s, flow speed = 80 μm/s, G_T = 7.0 °C/cm)

difference in the A-t plot (figure 4.c) before and after the flow was induced. But the difference is noticeable in log(A)-t plot (figure 4.d). The exponential growth rate (slope of log(A)-t curve) is slightly reduced after the initiation of the flow. However, whether this growth rate reduction is solely from the stabilizing effect of parallel flow or not is still an open question, because the nonlinearity could play a role in slowing down the growth (for the supercritical bifurcation) as the amplitude becomes larger and larger. Again the wavelength of the cellular interface is insensitive to the imposed parallel flow.

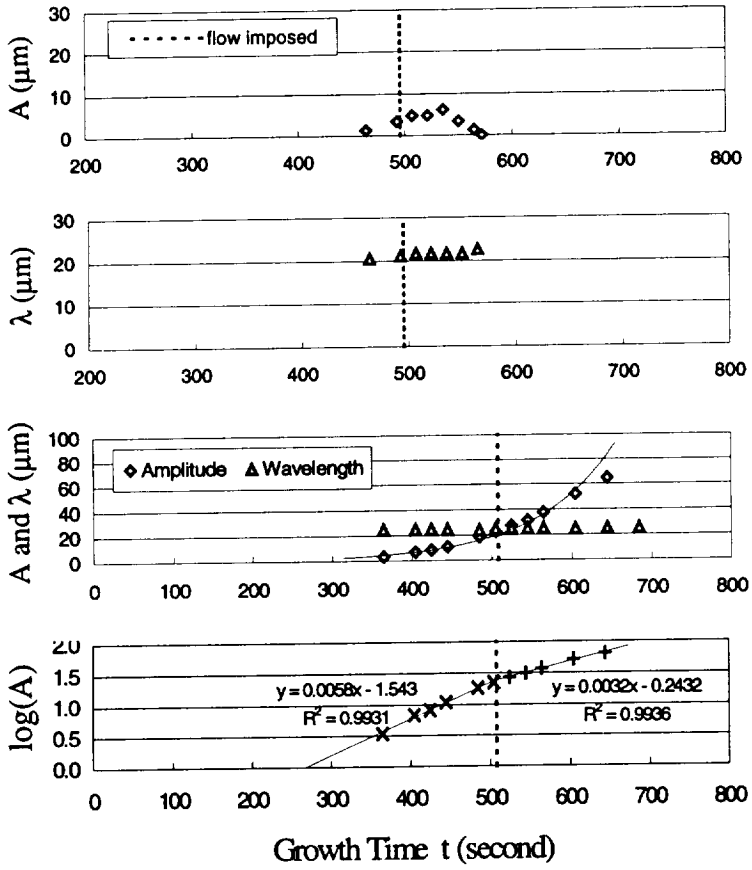

Figure 4 Effect of parallel shear flow on growth rate and wavelength (a,b,c,d, from top to bottom)

The physical mechanism explaining these observations is a version of that discussed by Dantzig and Chao[6] using a parallel shear flow model. Since the forced parallel flow does not affect the thermal transport, it influences the interface morphology by altering the solute transport. When the parallel shear flow is applied at an interface with small amplitudes (< 10 μm in the experiment), the flow field is minimally altered by the shallow cells and is still locally parallel to the interface. This local parallel flow dramatically enhances the lateral solute transport. Therefore the parallel flow when applied early stabilizes the interface by smoothing out the lateral solute inhomogeneity at the interface. However, when the parallel shear flow is applied at the deep cellular

interface, the flow field is distorted by the periodic curved interface and is no longer locally parallel to it. Flow has a stronger compressing effect on the upstream side of cells than the downstream side, which leads to an asymmetry in the concentration field with a thinner solutal boundary layer and greater concentration gradient G_c at the upstream side. Since G_c has a destabilizing effect on the interface, the upstream side of cell has a higher normal growth rate than the downstream side and as a result the cell tilts toward the incoming flow direction. It is proposed that it is the coupling effect between the interfacial morphology and the imposed parallel shear flow that leads to different crystal structures.

The interference pattern around a single crystal obtained in preliminary experiments is shown in figure 5. The originally paralleled interference fringes are distorted by the enrichment of the solute concentration as well as by the temperature gradient. This demonstrated the potential to make dynamic measurement of the solute field using an interference microscope. However, extra efforts are needed to properly resolve the interface in the interferogram.

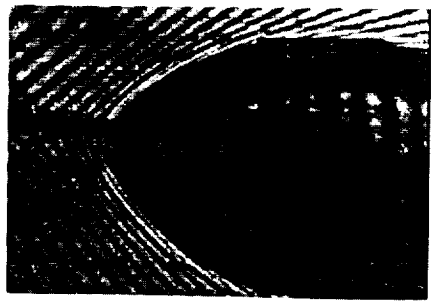

Figure 5 Interference pattern around a single crystal

Conclusion

The comparison of experimental data show that the parallel shear flow in a Hele-Shaw cell has a strong stabilizing effect on the planar interface by damping the existing initial perturbations. The flow also shows a stabilizing effect on the cellular interface by slightly reducing the exponential growth rate of cells. The left-right symmetry of cells is broken by the flow with cells tilting toward the incoming flow direction. The tilting angle increases with the velocity ratio. The experimental results are explained through the parallel flow effect on lateral solute transport. The phenomenon of cells tilting against the flow is consistent with the numerical result of Dantzig and Chao[6].

References

1. S. H. Davis, Handbook of Crystal Growth, 1B:861-897, 1993
2. R. T. Delves, J. Crystal Growth, 8:13-25, 1971
3. S. A. Forth and A. A. Wheeler, J. Fluid Mech., 202:339-366, 1989
4. S. A. Forth and A. A. Wheeler, J. Fluid Mech., 236:61-94, 1992
5. T. Huang, et al., J. Crystal Growth, 128:167-172, 1993
6. J. A. Dantzig and L. S. Chao, Proc. Instal. Symp. on Solidification Proc., 12-26,1990